

RoboBenchMart: Benchmarking Robots in Retail Environment

Konstantin Soshin*, Alexander Krapukhin*, Andrei Spiridonov*, Denis Shepelev†, Gregorii Bukhtuev, Andrey Kuznetsov, Vlad Shakhuro‡

FusionBrain Lab, Robotics Group

Abstract

Most existing robotic manipulation benchmarks focus on simplified tabletop scenarios, typically involving a stationary robotic arm interacting with various objects on a flat surface. To address this limitation, we introduce RoboBenchMart, a more challenging and realistic benchmark designed for dark store environments, where robots must perform complex manipulation tasks with diverse grocery items. This setting presents significant challenges, including dense object clutter and varied spatial configurations—with items positioned at different heights, depths, and in close proximity. By targeting the retail domain, our benchmark addresses a setting with strong potential for near-term automation impact. We demonstrate that current state-of-the-art generalist models struggle to solve even common retail tasks. To support further research, we release the **RoboBenchMart** suite, which includes a procedural store layout generator, a trajectory generation pipeline, evaluation tools and fine-tuned baseline models.

Page — <https://emb-ai.github.io/robobenchmart-project>

Code — <https://github.com/emb-ai/RoboBenchMart>

Data — <https://huggingface.co/emb-ai>

1 Introduction

Current robotic systems deployed in the real world mainly operate in constrained environments and typically perform a single, specific task. While these systems provide significant economic value, the true promise of future robotics lies in developing systems that can operate in unconstrained, noisy, and realistic settings, generalize across a wide range of variations, and perform multiple tasks. Recent advances in multimodal deep learning and robotics bring us closer to this goal; however, the widespread deployment of robots in unstructured, real-world settings remains a distant goal.

A promising application area where progress in robotics could enable large-scale deployment of robotic systems in the near future is the retail sector. In particular, dark stores have gained popularity worldwide in recent years. Dark stores are small retail distribution centers used to fulfill on-line orders. These stores are not open to the public; instead,

*These authors contributed equally.

†Project leader

‡Team leader



Figure 1: RoboBenchMart in action — the Fetch robot operates in a realistic, cluttered retail environment.

orders are collected by workers and delivered to customers. Consequently, the primary tasks performed by workers in dark stores are restocking and order picking.

We assume that the automation of retail tasks represents a realistic near-term goal due to several favorable factors. First, because dark store environments involve minimal interaction between robots and people, they impose fewer safety constraints. Second, these environments are more structured than conventional grocery stores, reducing the need for broad generalization and adaptation. Finally, such automation could benefit society by optimizing the flow of goods to end customers.

As testing robotic policies in the real world is challenging and expensive, a number of high-quality benchmarks have been developed in the recent years by the robotic research community. However, these benchmarks often focus on relatively simple tasks and fail to capture the full range of challenges and intricacies associated with retail environments. In particular, retail settings involve operation in cluttered spaces, a large variety of product items, multi-level shelving systems, and require advanced collision avoidance strategies to prevent damage to products, shelving, and the robot itself.

To address this gap and advance research in robotic re-

| Benchmark/ Dataset | Published in | Retail Domain | Scene Generation | Arrangement Generation | Release 3D Assets | Trajectories Generation | Tasks Diversity | Atomic Tasks | Composit. Tasks |
|-----------------------|-----------------|------------------|---------------------|---------------------------|----------------------|----------------------------|--------------------|-----------------|--------------------|
| ALFRED | CVPR'20 | ✗ | ✓ | ✓ | ✓ | ✓ | ✓ | ✓ | ✓ |
| RLBench | RA-L'19 | ✗ | ✗ | ✓ | ✓ | ✓ | ✓ | ✓ | ✓ |
| RoboCasa | RSS'24 | ✗ | ✓ | ✓ | ✓ | ✓ | ✓ | ✓ | ✓ |
| CALVIN | RA-L'22 | ✗ | ✗ | ✓ | n/a | ✓ | ✓ | ✓ | ✓ |
| LIBERO | NeurIPS'23 | ✗ | ✓ | ✓ | ✓ | ✓ | ✓ | ✓ | ✓ |
| VLABench | arXiv'24 | ✗ | ✓ | ✓ | ✓ | ✓ | ✓ | ✓ | ✓ |
| BEHAVIOR-1K | CoRL'22 | ✗ | ✗ | ✓ | ✓ | ✓ | ✓ | ✗ | ✓ |
| ManiSkill-HUB | ICLR'25 | ✗ | ✗ | ✓ | ✓ | ✓ | ✓ | ✓ | ✓ |
| RP2K | arXiv'20 | ✓ | ✗ | ✗ | ✗ | ✗ | ✗ | ✗ | ✗ |
| SKU110K | CVPR'19 | ✓ | ✗ | ✗ | ✗ | ✗ | ✗ | ✗ | ✗ |
| StandardSim | ICIAP'22 | ✓ | ✗ | ✓ | ✗ | ✗ | ✗ | ✗ | ✗ |
| IPA-3D1K | IROS'23 | ✓ | ✗ | ✓ | ✓ | ✗ | ✗ | ✗ | ✗ |
| FetchBot | arXiv'25 | ✓ | ✗ | ✓ | ✗ | ✓ | ✗ | ✓ | ✗ |
| RoboBenchMart | | ✓ | ✓ | ✓ | ✓ | ✓ | ✓ | ✓ | ✓ |

Table 1: Comparing proposed robotics retail benchmark with other benchmarks and datasets.

tail automation, we introduce **RoboBenchMart** — an open-source simulated retail benchmark suite designed to more accurately reflect the complexities of real-world retail tasks.

Overall, our main contributions are as follows:

- First, we introduce *Store Plan Generator*, an open procedural pipeline for generating realistic and diverse store layouts and product arrangements. It enables scalable creation of retail environments for training and evaluating robotic policies.
- Second, we present *Store Trajectories Sampler*, a pipeline that automatically collects trajectories for common retail tasks using motion planning and reinforcement learning methods. Moreover, we release a dataset of synthetic trajectories generated for the Fetch robot embodiment.
- Finally, we introduce *Store Robotics Benchmark*, to the best of our knowledge the first open benchmark dedicated to evaluating robotic policies in retail environments. Using our benchmark, we demonstrate that current state-of-the-art models struggle to complete typical retail tasks.

2 Related Work

2.1 Benchmarks and Datasets for Robotics

Inspired by the success of large-scale pretraining in CV (He et al. 2015; Dosovitskiy et al. 2021; Radford et al. 2021; Ravi et al. 2024) and NLP (Devlin et al. 2019; Brown et al. 2020; Touvron et al. 2023), robotics has pursued similar dataset development. However, collecting diverse and scalable robotic data remains challenging due to platform heterogeneity and physical interaction requirements (Collaboration et al. 2023; Khazatsky et al. 2024).

Real-world evaluation is also difficult to standardize, often requiring human resets and suffering from environment variability. As a result, simulation-based benchmarks have become popular for their reproducibility and ease of use.

Existing benchmarks mostly focus on household tasks. ALFRED (Shridhar et al. 2020), RLBench (James et al. 2020), RoboCasa (Nasiriany et al. 2024) and ManiSkill-HUB (Shukla, Tao, and Su 2025) offer tasks involving navigation, manipulation, and instruction following. Language-conditioned and lifelong learning are addressed in CALVIN (Mees et al. 2022), LIBERO (Liu et al. 2023), VLABench (Zhang et al. 2024), and BEHAVIOR-1K (Li et al. 2022).

However, retail and logistics scenarios — such as shelf picking or order packing — remain underexplored. Dedicated benchmarks for these domains are needed to advance robotic capabilities in retail environments.

2.2 Retail Domain

A number of datasets have been developed targeting retail-related computer vision tasks, including product classification (Peng, Xiao, and Li 2020), product detection (Goldman et al. 2019; Lindermayr et al. 2023), change detection and depth estimation (Mata et al. 2022).

Real-world datasets such as SKU110K (Goldman et al. 2019) and RP2K (Peng, Xiao, and Li 2020) are valuable for pretraining and evaluating the perception modules of robotic systems. However, they contain only 2D images of products and shelves, making them unsuitable for training or benchmarking robotic manipulation and navigation.

IPA-3D1K (Lindermayr et al. 2023) includes 1,000 high-quality 3D assets of real retail products, but it is not yet publicly available. The synthetic dataset StandardSim (Mata et al. 2022) offers only 2D image data, generated using 456 purchased product assets and a limited set of store layouts. Neither dataset provides code for generating scenes, product arrangements, or robotic trajectories, limiting their applicability to end-to-end robotics research.

FetchBot (Liu et al. 2025) introduces the UniVoxGen method for fast generation of highly cluttered shelf arrangements. However, it focuses solely on atomic picking task

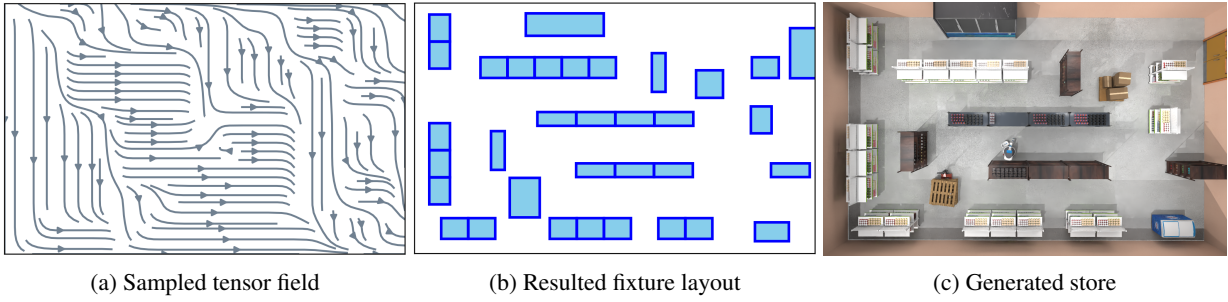


Figure 2: Examples of generated store with fixtures arranged by our pipeline.

and does not generate full store layouts or visualize product textures, which limits its applicability for benchmarking end-to-end robotic policies for retail.

In our work, we address these limitations by providing code to generate diverse store layouts and robotic trajectories, enabling the training and benchmarking of robotic policies in retail environments.

2.3 Trajectories Generation

Collecting robot trajectories via human teleoperation is costly and time-consuming (Liu et al. 2023; Zhang et al. 2024), while simulators offer privileged access to object states. As a result, automatic trajectory generation has become increasingly important.

Motion planning methods (e.g., RRT* (Karaman and Frazzoli 2011), CHOMP (Zucker et al. 2013)) can generate collision-free paths but require manual task specification, limiting their scalability. Reinforcement learning (RL) (Sutton and Barto 2018) learns from rewards (Haarnoja et al. 2018; Andrychowicz et al. 2021), but designing suitable reward functions is challenging, training is computationally intensive, and resulting behaviors may be suboptimal.

A promising alternative is demonstration-based augmentation. Methods like MimicGen (Mandlekar et al. 2023) scale a small set of human demonstrations by adapting them to new scenes, enabling diverse and reusable trajectory generation.

In our work, we demonstrate that standard motion planning and RL methods can be effectively leveraged to generate trajectories in retail store environments.

2.4 Robotic Models

Recent generalist models aim to unify perception and control across diverse tasks and robots. Octo (Octo Model Team et al. 2024), trained on 800k trajectories from 9 platforms, uses a transformer-based policy conditioned on goals via language or images. It generalizes well and can be quickly adapted to new embodiments. OpenVLA (Kim et al. 2024), a 7B Vision-Language-Action model, outperforms larger models like RT-2 on 29 manipulation tasks using multi-view visual features and a Llama-2 backbone. It supports efficient fine-tuning and strong multi-object reasoning. Pi0 (Black et al. 2024) combines a vision-language encoder with a flow-matching policy head. Trained on 68 tasks across multiple

robots, it adapts to new tasks with minimal data and supports varied embodiments, including mobile and dual-arm robots.

Despite strong results on household and tabletop tasks, these models remain untested in retail logistics. Real-world scenarios like warehouse picking or packing involve larger spaces, dynamic layouts, cluttered environments and time-critical demands. A dedicated benchmark is needed to evaluate how well such generalist policies transfer to retail environments.

3 Store Plan Generator

To emulate darkstore environments, our simulation scenes are designed as warehouse-like spaces containing shelving units and refrigerators arranged in various configurations. To facilitate domain randomization, we apply diverse textures to walls, floors, and ceilings, and incorporate multiple fixture designs. Product items are placed on the shelves in realistic, randomized positions.

3.1 Fixture Arrangement

Our store fixture arrangement pipeline is inspired by procedural street modeling (Chen et al. 2008) and consists of three main stages.

In the first **fixture random placement** stage, we generate a rectangular store area populated with randomly placed fixtures such as pallets, boxes, and freezers. Initial placement is performed using rejection sampling to ensure collision-free poses.

In the second stage, a **store tensor field** (Chen et al. 2008) is computed. Given an $N \times M$ square-meter store floor and a list of initial fixtures, we compute the tensor field as follows:

- (1) *Polygon Construction*: We extract polygons for the store floor and each already placed fixture. Each polygon is defined as a closed sequence of vertices $\{\mathbf{p}_i\}_{i=1}^P$, where each point \mathbf{p}_i is connected to \mathbf{p}_{i+1} , and for $i = P$, we define $\mathbf{p}_{P+1} := \mathbf{p}_1$. We also ensure that for all edge vectors $\mathbf{u}_i := \mathbf{p}_i - \mathbf{p}_{i+1}$, the condition $\|\mathbf{u}_i\| \leq D$ holds, where D denotes the maximum allowed edge length.
- (2) *Basis Tensor Field Computation*: For each point \mathbf{p}_i on the polygon, we compute a basis tensor: $T(\mathbf{p}) = l \begin{pmatrix} \cos 2\theta & \sin 2\theta \\ \sin 2\theta & -\cos 2\theta \end{pmatrix}$, where $l = \|\mathbf{u}_i\|$, $\theta = \arctan \frac{u_{ix}}{u_{iy}}$. This results in a set of basis tensors $\{T_j(\mathbf{p})\}$.

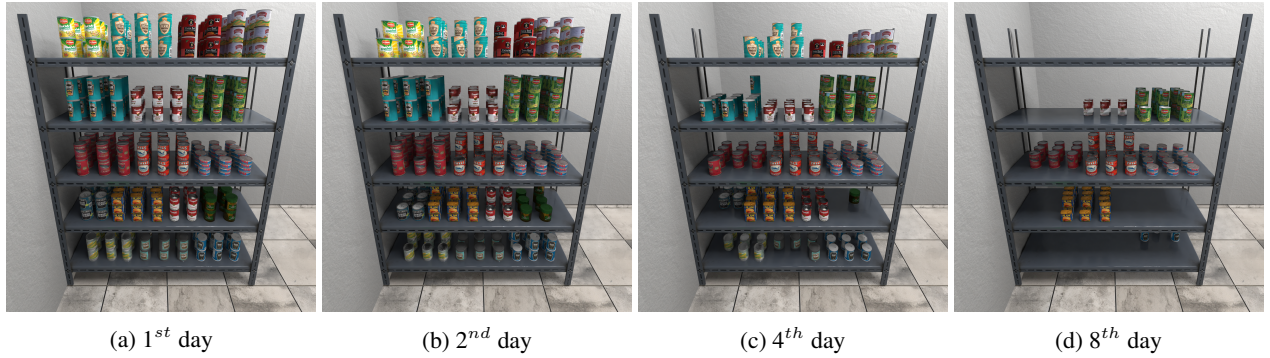


Figure 3: Example of product arrangement and shelf depletion over time produced by our simulator.



Figure 4: Examples of collected product assets.

- (3) *Tensor Field Aggregation*: The final tensor field over the store layout is computed as a weighted sum of the basis tensors: $T(\mathbf{p}) = \sum_j e^{-d\|\mathbf{p}-\mathbf{p}_j\|} T_j(\mathbf{p})$, where the weights decay exponentially with the distance from \mathbf{p} to the basis point \mathbf{p}_j , and the parameter $d > 0$ controls the rate of decay.

In the final **shelving unit arrangement** stage, shelves are placed according to the tensor field, ensuring alignment with local directions and maintaining a collision-free, navigable layout. Placement is performed in two passes: (1) *Horizontal pass*: Shelving units are placed row by row at positions where the tensor field indicates a horizontal orientation. (2) *Vertical pass*: Shelving units are placed column by column where the field indicates a vertical orientation. At each step, the local direction is interpolated from the pre-computed tensor grid, and placements are accepted only if they are collision-free and maintain the required passage width. Probabilistic skipping adds layout variability.

The proposed pipeline generates a structured and realistic store layout guided by the underlying sampled tensor field (see Figure 2).

3.2 Product Arrangement

To arrange products on shelves, we leverage the `scene_synthesizer` (Eppner et al. 2025) package, which automatically detects shelf surfaces suitable for item placement. Building on this framework, we implement a custom product placement module that positions items on a regular grid while introducing small pose perturbations

to simulate natural variability. The module also supports vertical stacking of items, as commonly observed in real stores. Additionally, it can leave empty spaces at the front of shelves using a Poisson process, simulating natural product depletion over time. Examples of product arrangements generated by our module are shown in Figure 3.

3.3 Assets and Textures

To represent 3D models of shelving units, refrigerators, and individual product items within our simulation environment, we utilize assets sourced from SketchFab¹. In total, we collected three shelving unit models, two refrigerator models, and 370 product assets across 21 categories (see Figure 4). Additionally, we gathered 26 floor, 17 wall, and 15 ceiling textures to support visual diversity in the generated store environments (see Figure 5). All assets and textures were verified to be licensed for unrestricted research use.

The collected 3D assets lacked consistent scale and orientation. We manually standardized their orientation and adjusted each model’s scale using reference dimensions obtained from online retail catalogs to ensure realistic proportions.

Furthermore, many original product meshes were unoptimized and contained excessive triangle counts, which significantly slowed rendering when scenes included hundreds of objects. To improve performance, we developed an automatic mesh simplification pipeline.

¹<https://sketchfab.com>



Figure 5: Examples of ceiling, wall, and floor textures used in our store generation pipeline, illustrating just a subset of possible variations.

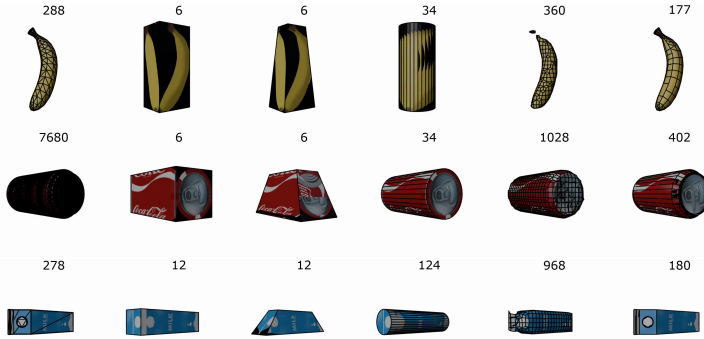


Figure 6: Example of different geometry approximations for assets (original on the left). Numbers above indicate face count for each mesh.

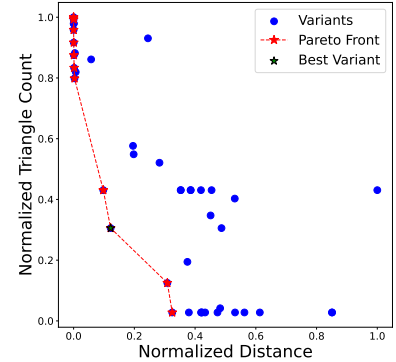


Figure 7: Variety of generated simplified meshes, Distance and Triangle Count are given in relative units (w.r.t max distance and initial triangle count).

Given the complexity of mesh decimation, an open research problem, we applied brute-force optimization across several heuristic methods, including QuadriFlow, Marching Cubes, and shape-specific approximations (e.g., cylinders, boxes), using the Blender Python API (see Figure 6).

From the Pareto-optimal set of remeshed outputs, we selected the version minimizing the total L_1 relative drop in geometry quality (measured by Chamfer distance) and maximizing triangle reduction (see Figure 7).

All collected and optimized assets are publicly available on https://huggingface.co/datasets/emb-ai/RoboBenchMart_assets.

4 Store Trajectories Sampler

In our Store Trajectory Sampler, we leverage both motion planning and reinforcement learning techniques to generate trajectory data. These trajectories can be used to train or fine-tune imitation learning policies.

4.1 Motion Planning

In our motion planning pipeline, we collect mobile manipulation trajectories as follows. For each task, we heuristically define a sequence of initial, intermediate, and final anchor poses. These poses are randomized to increase the diversity

of collected demonstrations. An example trajectory following anchor poses is shown in Figure 8.

Motion planning is carried out sequentially over the segments between successive anchor poses. To generate trajectories for each segment, we employ several algorithms.

For segments that do not require mobile base movement, we use a combination of screw motion (Murray, Li, and Sasthy 2017) and RRT-Connect (Kuffner and LaValle 2000). We first attempt to generate a trajectory using *screw motion*, which does not account for obstacles. The resulting trajectory is then checked for collisions. If it is unsafe, we next use slower *RRT-Connect*, which explicitly considers scene obstacles. If that trajectory is also invalid, the environment is reset. Otherwise, the trajectory is executed and the planner advances to the next segment.

For segments involving mobile base motion, we implement a set of task-specific heuristic planners that generate safe trajectories.

On average, our motion planning pipeline successfully produces feasible trajectories in 60% of cases across all tasks.



Figure 8: Examples of heuristically generated anchor poses used in our motion planner.

4.2 Reinforcement Learning

In our reinforcement learning setup, we train a separate policy for each task using privileged access to the full environment state. We adopt Proximal Policy Optimization (PPO) (Schulman et al. 2017) as the primary training algorithm, with manually crafted reward functions tailored to each task. These rewards typically include terms for proximity to the target product or pose, successful object placement, and avoidance of collisions with other items on shelves. On average, our reinforcement learning pipeline successfully produces feasible trajectories in 60% of cases across all tasks.

5 Store Robotics Benchmark

The goal of our benchmark is to evaluate the capabilities of current state-of-the-art generalist policies in retail environments, with fine-tuning using generated trajectories. It is built on ManiSkill3 (Tao et al. 2025), a high-performance robot simulation framework with realistic physics and ray-traced rendering. We use the Fetch robot (Figure 1), a mobile manipulator with a differential-drive base, a 7-DOF arm, and a prismatic torso joint for vertical reach. Its parallel gripper enables versatile object manipulation in dynamic settings.

5.1 Testing Scenarios

To assess the generalization capabilities of policies fine-tuned within our benchmark, we consider the following axes of environment and task variation:

1. *Robot Position*: Randomized start positions within task-relevant regions. Used during training trajectory generation.
2. *Textures*: Random variations in wall, floor, ceiling, and door textures. Present during training.
3. *Store Layout*: Unseen store layouts at test time represent an out-of-distribution (OOD) domain.
4. *Unseen Shelf Arrangement*: Shelf arrangements not encountered during training.
5. *Unseen in Task Items*: Items encountered during training in other tasks but not in the target task. Considered OOD with respect to the specific task.
6. *Completely Unseen Items*: Items not encountered during training at all. Represents a more challenging form of OOD.

To balance benchmarking feasibility with meaningful generalization evaluation, we define the following testing scenarios:

- **In-Domain**: Robot position randomization only (1).
- **Unseen Scenes**: Robot position, texture, and store layout randomization (1 + 2 + 3).
- **Unseen Scenes & Items**: Unseen scenes with additional OOD items drawn from other tasks (1 + 2 + 3 + 5).

Although our benchmark supports scenarios 4 and 6, we exclude them from evaluation, as current policies consistently fail even under the simpler conditions considered above (see Table 2).

These configurations allow us to evaluate policy generalization across increasingly challenging deployment conditions, including novel scene layouts and object combinations.

5.2 Tasks

We design a set of atomic tasks covering fundamental manipulation skills required to accomplish retail-related objectives:

- **Pick to basket** — the robot must pick an item from a shelf or refrigerator and place it into a cart.
- **Pick from floor** — an item that has fallen to the floor must be picked up and returned to its appropriate location.
- **From board to board** — the robot transfers an item from one board to another.
- **Open fridge** — the robot opens the door of a refrigerator.
- **Close fridge** — the robot closes the door of a refrigerator.

Building on atomic tasks, we define composite tasks:

- **Pick {N} items** — the robot is provided with a list of N items and must collect all specified products and place them in the cart.
- **Pick from fridge** — open the fridge, pick an item, and close the fridge.

Each task includes a textual instruction specifying the target item and fixture names. The robot is expected to interact with the nearest matching instances, as no specific objects are explicitly designated. When assessing task completion, we evaluate not only the final positions of target products and fixtures, but also verify that surrounding items were not disturbed or collided with during policy execution.

5.3 Generalist Baselines

We evaluate three state-of-the-art generalist VLA models: lightweight transformer Octo (Octo Model Team et al. 2024) and LLM-based π_0 (Black et al. 2024) and $\pi_{0.5}$ (Black et al.

| Model | Param. (#) | Testing scenario | Atomic Tasks | | | | | Composite Tasks | |
|-------------|------------|-----------------------|----------------|-----------------|---------------------|-------------|--------------|-----------------|------------------|
| | | | Pick to basket | Pick from floor | From board to board | Open fridge | Close fridge | Pick 3 items | Pick from fridge |
| Octo | 93M | In-Domain | 17 | 2 | 13 | 32 | 41 | 0 | 0 |
| | | Unseen Scenes | 1 | 0 | 2 | 10 | 37 | 0 | 0 |
| | | Unseen Scenes & Items | 0 | 0 | 0 | n/a | n/a | 0 | 0 |
| π_0 | 3.3B | In-Domain | 22 | 29 | 15 | 48 | 83 | 0 | 0 |
| | | Unseen Scenes | 1 | 12 | 5 | 25 | 75 | 0 | 0 |
| | | Unseen Scenes & Items | 0 | 0 | 0 | n/a | n/a | 0 | 0 |
| $\pi_{0.5}$ | 3.3B | In-Domain | 63 | 44 | 55 | 50 | 85 | 0 | 0 |
| | | Unseen Scenes | 38 | 11 | 22 | 37 | 77 | 0 | 0 |
| | | Unseen Scenes & Items | 10 | 0 | 23 | n/a | n/a | 0 | 0 |

Table 2: Average success rates (%) of generalist VLA models on atomic and composite retail tasks across different testing scenarios. Higher values indicate better performance. n/a indicate that scenario is not applicable for the task.

2025). Each model is fine-tuned via imitation learning using trajectories generated by our Store Trajectory Sampler.

To reduce computational overhead and preserve the fine-tuning setup, we generate only 248 trajectories per (task, item, fixture) triplet, totaling 2,480 demonstrations. To evaluate generalization, we limit the number of training objects per task to 2–3, ensuring they remain unseen in all other tasks. Although our simulator supports a variety of item arrangements, we use fully packed shelves for both training and testing (Figure 3a), as models already struggle under this simplified configuration. Further details on the collected trajectories can be found in Appendix A.

Models are finetuned exclusively on atomic tasks. Composite tasks are evaluated by decomposing them into sequences of atomic instructions, executed step by step using the same policy. Further details on fine-tuning and hyperparameters are provided in Appendix B.

5.4 Evaluation Results

Evaluation results are presented in Table 2. We evaluate performance on atomic and composite tasks using the mean success rate per task. We use 50 trials per (task, item, fixture) triplet to estimate success rates. Detailed evaluation results and failure mode analysis are presented in Appendix C.

The results in Table 2 show that **current generalist VLA models struggle even with basic retail tasks**. Octo performs poorly across all scenarios, while π_0 performs moderately in the In-Domain setting but deteriorates in Unseen Scenes and fails completely in the Unseen Scenes & Items condition. $\pi_{0.5}$ performs significantly better and is the only model that achieves non-zero success rates in the Unseen Scenes & Items scenario, though it remains far from reliable. Composite task performance is zero for all models, indicating a limited ability to execute multi-step instructions or generalize across stages.

These results highlight key limitations of existing generalist models: **fragility to minor scene changes** (e.g., layouts, textures, object placements), **poor generalization from limited demonstrations** to novel object-task combinations, and **inadequate support for long-horizon, compositional ex-**

cution. Our findings suggest that existing **pretrained models may be insufficient** for effective application in the retail domain, and that **targeted pretraining on retail-specific data may be necessary**.

6 Limitations and Future Work

While RoboBenchMart provides a realistic and diverse environment for evaluating robotic policies in retail settings, several limitations remain.

1. Our benchmark supports only a parallel-jaw gripper and does not model suction-based end-effectors, which are widely used in warehouse automation, or dexterous multi-fingered hands, developed for humanoid robots.
2. Some wide or irregularly shaped packages cannot be grasped by the Fetch gripper. Additionally, to ensure reliable grasping, product arrangements include relatively large gaps between items. While these constraints limit realism, they may reflect practical design choices in future dark stores, where item packaging and shelf layout could be standardized to better accommodate robotic manipulation.
3. The benchmark includes only rigid-body packages, omitting deformable items that present unique manipulation challenges. Incorporating such objects would enhance real-world variability and enable better assessment of generalization.

Addressing these limitations is an important step toward improving the realism, scope, and utility of the benchmark. Another key direction for future work is to develop new tasks that broaden the benchmark’s scope and introduce more challenging evaluation scenarios. We plan to incorporate these improvements in future versions of the benchmark.

7 Conclusion

In this work, we introduced a novel open-source RoboBenchMart suite for benchmarking robotic systems in retail environments, a domain with significant practical relevance and underexplored challenges. The suite includes

a procedural store layout generator, a trajectory generation pipeline, evaluation tools, and fine-tuned baseline models. Our experiments show that current state-of-the-art generalist models struggle with common retail scenarios, highlighting a clear mismatch between existing capabilities and the demands of real-world automation. We hope our work will facilitate the development of more robust, scalable, and task-aware robotic systems. All components of RoboBench-Mart are publicly available to support future research in this direction.

References

- Andrychowicz, M.; Raichuk, A.; Stańczyk, P.; Orsini, M.; Girgin, S.; Marinier, R.; Hussenot, L.; Geist, M.; Pietquin, O.; Michalski, M.; Gelly, S.; and Bachem, O. 2021. What Matters In On-Policy Reinforcement Learning? A Large-Scale Empirical Study. In *ICLR 2021 - Ninth International Conference on Learning Representations*. Vienna / Virtual, Austria.
- Black, K.; Brown, N.; Darpinian, J.; Dhabalia, K.; Driess, D.; Esmail, A.; Equi, M.; Finn, C.; Fusai, N.; Galliker, M. Y.; Ghosh, D.; Groom, L.; Hausman, K.; Ichter, B.; Jakubczak, S.; Jones, T.; Ke, L.; LeBlanc, D.; Levine, S.; Li-Bell, A.; Mothukuri, M.; Nair, S.; Pertsch, K.; Ren, A. Z.; Shi, L. X.; Smith, L.; Springenberg, J. T.; Stachowicz, K.; Tanner, J.; Vuong, Q.; Walke, H.; Walling, A.; Wang, H.; Yu, L.; and Zhilinsky, U. 2025. $\pi_{0.5}$: a Vision-Language-Action Model with Open-World Generalization. arXiv:2504.16054.
- Black, K.; Brown, N.; Driess, D.; Esmail, A.; Equi, M.; Finn, C.; Fusai, N.; Groom, L.; Hausman, K.; Ichter, B.; Jakubczak, S.; Jones, T.; Ke, L.; Levine, S.; Li-Bell, A.; Mothukuri, M.; Nair, S.; Pertsch, K.; Shi, L. X.; Tanner, J.; Vuong, Q.; Walling, A.; Wang, H.; and Zhilinsky, U. 2024. π_0 : A Vision-Language-Action Flow Model for General Robot Control. arXiv:2410.24164.
- Brown, T.; Mann, B.; Ryder, N.; Subbiah, M.; Kaplan, J. D.; Dhariwal, P.; Neelakantan, A.; Shyam, P.; Sastry, G.; Askell, A.; Agarwal, S.; Herbert-Voss, A.; Krueger, G.; Henighan, T.; Child, R.; Ramesh, A.; Ziegler, D.; Wu, J.; Winter, C.; Hesse, C.; Chen, M.; Sigler, E.; Litwin, M.; Gray, S.; Chess, B.; Clark, J.; Berner, C.; McCandlish, S.; Radford, A.; Sutskever, I.; and Amodei, D. 2020. Language Models are Few-Shot Learners. In Larochelle, H.; Ranzato, M.; Hadsell, R.; Balcan, M.; and Lin, H., eds., *Advances in Neural Information Processing Systems*, volume 33, 1877–1901. Curran Associates, Inc.
- Chen, G.; Esch, G.; Wonka, P.; Müller, P.; and Zhang, E. 2008. Interactive procedural street modeling. *ACM Trans. Graph.*, 27(3): 1–10.
- Clark, J. H. 1976. Hierarchical geometric models for visible surface algorithms. *Communications of the ACM*, 19(10): 547–554.
- Collaboration, O. X.-E.; O’Neill, A.; Rehman, A.; Gupta, A.; Maddukuri, A.; Gupta, A.; Padalkar, A.; Lee, A.; Pooley, A.; Gupta, A.; Mandlekar, A.; Jain, A.; Tung, A.; Bewley, A.; Herzog, A.; Irpan, A.; Khazatsky, A.; Rai, A.; Gupta, A.; Wang, A.; Kolobov, A.; Singh, A.; Garg, A.; Kembhavi, A.; Xie, A.; Brohan, A.; Raffin, A.; Sharma, A.; Yavary, A.; Jain, A.; Balakrishna, A.; Wahid, A.; Burgess-Limerick, B.; Kim, B.; Schölkopf, B.; Wulfe, B.; Ichter, B.; Lu, C.; Xu, C.; Le, C.; Finn, C.; Wang, C.; Xu, C.; Chi, C.; Huang, C.; Chan, C.; Agia, C.; Pan, C.; Fu, C.; Devin, C.; Xu, D.; Morton, D.; Driess, D.; Chen, D.; Pathak, D.; Shah, D.; Büchler, D.; Jayaraman, D.; Kalashnikov, D.; Sadigh, D.; Johns, E.; Foster, E.; Liu, F.; Ceola, F.; Xia, F.; Zhao, F.; Frujeri, F. V.; Stulp, F.; Zhou, G.; Sukhatme, G. S.; Salhotra, G.; Yan, G.; Feng, G.; Schiavi, G.; Berseth, G.; Kahn, G.; Yang, G.; Wang, G.; Su, H.; Fang, H.-S.; Shi, H.; Bao, H.; Amor, H. B.; Christensen, H. I.; Furuta, H.; Bharadhwaj, H.; Walke, H.; Fang, H.; Ha, H.; Mordatch, I.; Radosavovic, I.; Leal, I.; Liang, J.; Abou-Chakra, J.; Kim, J.; Drake, J.; Peters, J.; Schneider, J.; Hsu, J.; Vakil, J.; Bohg, J.; Bingham, J.; Wu, J.; Gao, J.; Hu, J.; Wu, J.; Wu, J.; Sun, J.; Luo, J.; Gu, J.; Tan, J.; Oh, J.; Wu, J.; Lu, J.; Yang, J.; Malik, J.; Silvério, J.; Hejna, J.; Booher, J.; Tompson, J.; Yang, J.; Salvador, J.; Lim, J. J.; Han, J.; Wang, K.; Rao, K.; Pertsch, K.; Hausman, K.; Go, K.; Gopalakrishnan, K.; Goldberg, K.; Byrne, K.; Oslund, K.; Kawaharazuka, K.; Black, K.; Lin, K.; Zhang, K.; Ehsani, K.; Lekkala, K.; Ellis, K.; Rana, K.; Srinivasan, K.; Fang, K.; Singh, K. P.; Zeng, K.-H.; Hatch, K.; Hsu, K.; Itti, L.; Chen, L. Y.; Pinto, L.; Fei-Fei, L.; Tan, L.; Fan, L. J.; Ott, L.; Lee, L.; Weihs, L.; Chen, M.; Lepert, M.; Memmel, M.; Tomizuka, M.; Itkina, M.; Castro, M. G.; Spero, M.; Du, M.; Ahn, M.; Yip, M. C.; Zhang, M.; Ding, M.; Heo, M.; Srirama, M. K.; Sharma, M.; Kim, M. J.; Irshad, M. Z.; Kanazawa, N.; Hansen, N.; Heess, N.; Joshi, N. J.; Suenderhauf, N.; Liu, N.; Palo, N. D.; Shafiuallah, N. M. M.; Mees, O.; Kroemer, O.; Bastani, O.; Sanketi, P. R.; Miller, P. T.; Yin, P.; Wohlhart, P.; Xu, P.; Fagan, P. D.; Mirano, P.; Sermanet, P.; Abbeel, P.; Sundaresan, P.; Chen, Q.; Vuong, Q.; Rafailov, R.; Tian, R.; Doshi, R.; Mart’ in Mart’ in, R.; Bajjal, R.; Scalise, R.; Hendrix, R.; Lin, R.; Qian, R.; Zhang, R.; Mendonca, R.; Shah, R.; Hoque, R.; Julian, R.; Bustamante, S.; Kirmani, S.; Levine, S.; Lin, S.; Moore, S.; Bahl, S.; Dass, S.; Sonawani, S.; Tulsiani, S.; Song, S.; Xu, S.; Haldar, S.; Karamcheti, S.; Adebola, S.; Guist, S.; Nasiriany, S.; Schaal, S.; Welker, S.; Tian, S.; Ramamoorthy, S.; Dasari, S.; Belkhale, S.; Park, S.; Nair, S.; Mirchandani, S.; Osa, T.; Gupta, T.; Harada, T.; Matsushima, T.; Xiao, T.; Kollar, T.; Yu, T.; Ding, T.; Davchev, T.; Zhao, T. Z.; Armstrong, T.; Darrell, T.; Chung, T.; Jain, V.; Kumar, V.; Vanhoucke, V.; Guizilini, V.; Zhan, W.; Zhou, W.; Burgard, W.; Chen, X.; Chen, X.; Wang, X.; Zhu, X.; Geng, X.; Liu, X.; Liangwei, X.; Li, X.; Pang, Y.; Lu, Y.; Ma, Y. J.; Kim, Y.; Chebotar, Y.; Zhou, Y.; Zhu, Y.; Wu, Y.; Xu, Y.; Wang, Y.; Bisk, Y.; Dou, Y.; Cho, Y.; Lee, Y.; Cui, Y.; Cao, Y.; Wu, Y.-H.; Tang, Y.; Zhu, Y.; Zhang, Y.; Jiang, Y.; Li, Y.; Li, Y.; Iwasawa, Y.; Matsuo, Y.; Ma, Z.; Xu, Z.; Cui, Z. J.; Zhang, Z.; Fu, Z.; and Lin, Z. 2023. Open X-Embodiment: Robotic Learning Datasets and RT-X Models. <https://arxiv.org/abs/2310.08864>.
- Devlin, J.; Chang, M.-W.; Lee, K.; and Toutanova, K. 2019. BERT: Pre-training of Deep Bidirectional Transformers for Language Understanding. arXiv:1810.04805.
- Dosovitskiy, A.; Beyer, L.; Kolesnikov, A.; Weissenborn,

- D.; Zhai, X.; Unterthiner, T.; Dehghani, M.; Minderer, M.; Heigold, G.; Gelly, S.; Uszkoreit, J.; and Hounsby, N. 2021. An Image is Worth 16x16 Words: Transformers for Image Recognition at Scale. *ICLR*.
- Eppner, C.; Murali, A.; Garrett, C.; O’Flaherty, R.; Hermans, T.; Yang, W.; and Fox, D. 2025. scene_synthesizer: A Python Library for Procedural Scene Generation in Robot Manipulation. *Journal of Open Source Software*, 10(105): 7561.
- Goldman, E.; Herzig, R.; Eisenschtat, A.; Goldberger, J.; and Hassner, T. 2019. Precise detection in densely packed scenes. In *Proceedings of the IEEE/CVF conference on computer vision and pattern recognition*, 5227–5236.
- Haarnoja, T.; Zhou, A.; Abbeel, P.; and Levine, S. 2018. Soft actor-critic: Off-policy maximum entropy deep reinforcement learning with a stochastic actor. In *International conference on machine learning*, 1861–1870. Pmlr.
- He, K.; Zhang, X.; Ren, S.; and Sun, J. 2015. Deep Residual Learning for Image Recognition. *arXiv preprint arXiv:1512.03385*.
- James, S.; Ma, Z.; Rovick Arrojo, D.; and Davison, A. J. 2020. RL-Bench: The Robot Learning Benchmark & Learning Environment. *IEEE Robotics and Automation Letters*.
- Karaman, S.; and Frazzoli, E. 2011. Sampling-based algorithms for optimal motion planning. *The International Journal of Robotics Research*, 30(7): 846–894.
- Khazatsky, A.; Pertsch, K.; Nair, S.; Balakrishna, A.; Dasari, S.; Karamcheti, S.; Nasiriany, S.; Srirama, M. K.; Chen, L. Y.; Ellis, K.; Fagan, P. D.; Hejna, J.; Itkina, M.; Lepert, M.; Ma, Y. J.; Miller, P. T.; Wu, J.; Belkhale, S.; Dass, S.; Ha, H.; Jain, A.; Lee, A.; Lee, Y.; Memmel, M.; Park, S.; Radosavovic, I.; Wang, K.; Zhan, A.; Black, K.; Chi, C.; Hatch, K. B.; Lin, S.; Lu, J.; Mercat, J.; Rehman, A.; Sanketi, P. R.; Sharma, A.; Simpson, C.; Vuong, Q.; Walke, H. R.; Wulfe, B.; Xiao, T.; Yang, J. H.; Yavary, A.; Zhao, T. Z.; Agia, C.; Baijal, R.; Castro, M. G.; Chen, D.; Chen, Q.; Chung, T.; Drake, J.; Foster, E. P.; Gao, J.; Guizilini, V.; Herrera, D. A.; Heo, M.; Hsu, K.; Hu, J.; Irshad, M. Z.; Jackson, D.; Le, C.; Li, Y.; Lin, K.; Lin, R.; Ma, Z.; Maddukuri, A.; Mirchandani, S.; Morton, D.; Nguyen, T.; O’Neill, A.; Scalise, R.; Seale, D.; Son, V.; Tian, S.; Tran, E.; Wang, A. E.; Wu, Y.; Xie, A.; Yang, J.; Yin, P.; Zhang, Y.; Bastani, O.; Berseth, G.; Bohg, J.; Goldberg, K.; Gupta, A.; Gupta, A.; Jayaraman, D.; Lim, J. J.; Malik, J.; Martín-Martín, R.; Ramamoorthy, S.; Sadigh, D.; Song, S.; Wu, J.; Yip, M. C.; Zhu, Y.; Kollar, T.; Levine, S.; and Finn, C. 2024. DROID: A Large-Scale In-The-Wild Robot Manipulation Dataset. *RSS 2024 Workshop: Data Generation for Robotics*.
- Kim, M.; Pertsch, K.; Karamcheti, S.; Xiao, T.; Balakrishna, A.; Nair, S.; Rafailov, R.; Foster, E.; Lam, G.; Sanketi, P.; Vuong, Q.; Kollar, T.; Burchfiel, B.; Tedrake, R.; Sadigh, D.; Levine, S.; Liang, P.; and Finn, C. 2024. OpenVLA: An Open-Source Vision-Language-Action Model. *arXiv preprint arXiv:2406.09246*.
- Kuffner, J. J.; and LaValle, S. M. 2000. RRT-connect: An efficient approach to single-query path planning. In *Proceedings 2000 ICRA. Millennium conference. IEEE international conference on robotics and automation. Symposia proceedings (Cat. No. 00CH37065)*, volume 2, 995–1001. IEEE.
- Li, C.; Zhang, R.; Wong, J.; Gokmen, C.; Srivastava, S.; Martín-Martín, R.; Wang, C.; Levine, G.; Lingelbach, M.; Sun, J.; Anvari, M.; Hwang, M.; Sharma, M.; Aydin, A.; Bansal, D.; Hunter, S.; Kim, K.-Y.; Lou, A.; Matthews, C. R.; Villa-Renteria, I.; Tang, J. H.; Tang, C.; Xia, F.; Savarese, S.; Gweon, H.; Liu, K.; Wu, J.; and Fei-Fei, L. 2022. BEHAVIOR-1K: A Benchmark for Embodied AI with 1,000 Everyday Activities and Realistic Simulation. In *6th Annual Conference on Robot Learning*.
- Lindermayr, J.; Odabasi, C.; Jordan, F.; Graf, F.; Knak, L.; Kraus, W.; Bormann, R.; and Huber, M. F. 2023. IPA-3D1K: a large retail 3D model dataset for robot picking. In *2023 IEEE/RSJ International Conference on Intelligent Robots and Systems (IROS)*, 11404–11411. IEEE.
- Liu, B.; Zhu, Y.; Gao, C.; Feng, Y.; Liu, Q.; Zhu, Y.; and Stone, P. 2023. Libero: Benchmarking knowledge transfer for lifelong robot learning. *Advances in Neural Information Processing Systems*, 36: 44776–44791.
- Liu, W.; Wan, Y.; Wang, J.; Kuang, Y.; Shi, X.; Li, H.; Zhao, D.; Zhang, Z.; and Wang, H. 2025. FetchBot: Object Fetching in Cluttered Shelves via Zero-Shot Sim2Real. *arXiv preprint arXiv:2502.17894*.
- Mandlekar, A.; Nasiriany, S.; Wen, B.; Akinola, I.; Narang, Y.; Fan, L.; Zhu, Y.; and Fox, D. 2023. MimicGen: A Data Generation System for Scalable Robot Learning using Human Demonstrations. In *7th Annual Conference on Robot Learning*.
- Mata, C.; Locascio, N.; Sheikh, M. A.; Kihara, K.; and Fischetti, D. 2022. Standardsim: A synthetic dataset for retail environments. In *International Conference on Image Analysis and Processing*, 65–76. Springer.
- Mees, O.; Hermann, L.; Rosete-Beas, E.; and Burgard, W. 2022. CALVIN: A Benchmark for Language-Conditioned Policy Learning for Long-Horizon Robot Manipulation Tasks. *IEEE Robotics and Automation Letters (RA-L)*, 7(3): 7327–7334.
- Murray, R. M.; Li, Z.; and Sastry, S. S. 2017. *A mathematical introduction to robotic manipulation*. CRC press.
- Nasiriany, S.; Maddukuri, A.; Zhang, L.; Parikh, A.; Lo, A.; Joshi, A.; Mandlekar, A.; and Zhu, Y. 2024. RoboCasa: Large-Scale Simulation of Everyday Tasks for Generalist Robots. In *Robotics: Science and Systems*.
- Octo Model Team; Ghosh, D.; Walke, H.; Pertsch, K.; Black, K.; Mees, O.; Dasari, S.; Hejna, J.; Xu, C.; Luo, J.; Kreiman, T.; Tan, Y.; Chen, L. Y.; Sanketi, P.; Vuong, Q.; Xiao, T.; Sadigh, D.; Finn, C.; and Levine, S. 2024. Octo: An Open-Source Generalist Robot Policy. In *Proceedings of Robotics: Science and Systems*. Delft, Netherlands.
- Peng, J.; Xiao, C.; and Li, Y. 2020. RP2K: A large-scale retail product dataset for fine-grained image classification. *arXiv preprint arXiv:2006.12634*.
- Radford, A.; Kim, J. W.; Hallacy, C.; Ramesh, A.; Goh, G.; Agarwal, S.; Sastry, G.; Askell, A.; Mishkin, P.; Clark, J.; Krueger, G.; and Sutskever, I. 2021. Learning Transferable Visual Models From Natural Language Supervision. In

Meila, M.; and Zhang, T., eds., *Proceedings of the 38th International Conference on Machine Learning*, volume 139 of *Proceedings of Machine Learning Research*, 8748–8763. PMLR.

Ravi, N.; Gabeur, V.; Hu, Y.-T.; Hu, R.; Ryali, C.; Ma, T.; Khedr, H.; Rädle, R.; Rolland, C.; Gustafson, L.; Mintun, E.; Pan, J.; Alwala, K. V.; Carion, N.; Wu, C.-Y.; Girshick, R.; Dollár, P.; and Feichtenhofer, C. 2024. SAM 2: Segment Anything in Images and Videos. *arXiv preprint arXiv:2408.00714*.

Schulman, J.; Wolski, F.; Dhariwal, P.; Radford, A.; and Klimov, O. 2017. Proximal policy optimization algorithms. *arXiv preprint arXiv:1707.06347*.

Shridhar, M.; Thomason, J.; Gordon, D.; Bisk, Y.; Han, W.; Mottaghi, R.; Zettlemoyer, L.; and Fox, D. 2020. ALFRED: A Benchmark for Interpreting Grounded Instructions for Everyday Tasks. In *The IEEE Conference on Computer Vision and Pattern Recognition (CVPR)*.

Shukla, A.; Tao, S.; and Su, H. 2025. ManiSkill-HAB: A Benchmark for Low-Level Manipulation in Home Rearrangement Tasks. In *ICLR 2025 - 13th International Conference on Learning Representations*.

Sutton, R. S.; and Barto, A. G. 2018. *Reinforcement Learning: An Introduction*. Cambridge, MA: MIT Press, 2nd edition. ISBN 9780262039246.

Tao, S.; Xiang, F.; Shukla, A.; Qin, Y.; Hinrichsen, X.; Yuan, X.; Bao, C.; Lin, X.; Liu, Y.; Chan, T.-K.; et al. 2025. ManiSkill3: GPU Parallelized Robot Simulation and Rendering for Generalizable Embodied AI. In *7th Robot Learning Workshop: Towards Robots with Human-Level Abilities*.

Touvron, H.; Lavril, T.; Izacard, G.; Martinet, X.; Lachaux, M.-A.; Lacroix, T.; Rozière, B.; Goyal, N.; Hambro, E.; Azhar, F.; Rodriguez, A.; Joulin, A.; Grave, E.; and Lample, G. 2023. LLaMA: Open and Efficient Foundation Language Models. *arXiv:2302.13971*.

Zhang, S.; Xu, Z.; Liu, P.; Yu, X.; Li, Y.; Gao, Q.; Fei, Z.; Yin, Z.; Wu, Z.; Jiang, Y.-G.; and Qiu, X. 2024. VLABench: A Large-Scale Benchmark for Language-Conditioned Robotics Manipulation with Long-Horizon Reasoning Tasks. *arXiv:2412.18194*.

Zucker, M.; Ratliff, N.; Dragan, A. D.; Pivtoraiko, M.; Klingsmith, M.; Dellin, C. M.; Bagnell, J. A.; and Srinivasa, S. S. 2013. CHOMP: Covariant Hamiltonian optimization for motion planning. *The International Journal of Robotics Research*, 32(9-10): 1164–1193.

A Tasks and Datasets

A.1 Atomic Tasks

We define five atomic tasks encompassing two core manipulation skills: (1) *pick and place*, (2) *open/close* doors. Task details are outlined in Table 3. At the start of each episode, the robot’s initial pose is randomized near the target shelf or fridge.

To assess generalization in *pick and place* tasks, we selected a subset of eight product items and partitioned them into train/test splits. For each task, test items were excluded

from training on that specific task but were present in the training set of other tasks. See Table 4 for the full item distribution.

A.2 Composite Tasks

To evaluate the models’ ability to execute multiple atomic tasks sequentially, we designed two long-horizon tasks. The first, *Pick 3 items*, requires the robot to perform the *Pick to basket* task for three different items in sequence. The second task, *Pick from fridge*, simulates a scenario where the robot must retrieve an item from a closed refrigerated showcase. This task comprises three atomic subtasks: *Open fridge*, *Pick to basket*, and *Close fridge*.

We evaluate policies in the long-horizon setup using an oracle that decomposes each composite task into a sequence of atomic subtasks, executed sequentially upon the successful completion of the preceding subtask.

A.3 Training Dataset



Figure 9: Examples of input images used during training and evaluation.

To obtain demonstration trajectories we employed motion planning algorithms from `mplib`² package. We collected 248 demonstration trajectories per train object for *pick and place* tasks and 248 per *open/close* tasks. A total of 2,976 trajectories were collected, comprising 1,401,169 transitions. The whole process of data generation (scene synthesis, motion planning and camera rendering) takes approximately 8 hours on an NVIDIA V100 GPU.

In the main paper, we mistakenly reported that we collected 2,480 trajectories. This count omitted an additional 496 trajectories related to the “opening and closing showcase” task. The correct total is 2,976 trajectories. We will update the paper to reflect this upon acceptance.

Our training data comprises the following components:

1. Observations, including:

- **Textual command:** describes the task to perform along with the target objects.
- **Images:** RGB views from the left shoulder camera (256×256×3), gripper camera (128×128×3), and right shoulder camera (256×256×3) (see Figure 9). Note that we did not employ images captured from the native Fetch head camera, as this view is usually blocked by the robot’s hand.
- **Proprioception:** joint positions and velocities.

²<https://motion-planning-lib.readthedocs.io/latest/>

| Task | Skill Family | Description | Success Criteria | Language instruction example |
|---------------------|----------------|---|---|---|
| Pick to basket | Pick and place | Pick an object with specified name from the shelf and place it in the basket. | Any object of the target type is inside the basket, other items are not moved, the robot is static. | move to the shelf, pick the fanta bottle, and place it in the basket |
| Pick from floor | Pick and place | Pick an object from the floor and place it to the target shelf (the second or the third board). | The object is placed near the correct group of products, other items are not moved, and the robot remains static. | pick the SLAM luncheon meat from the floor and place it on the shelf |
| From board to board | Pick and place | Pick an object with the specified name from one board and place it one board higher (from the second board to the third, or from the third to the fourth). The target board is empty. | The object is placed near the correct group of products, other items are not moved, the robot is static. | pick the Duff Beer Can and place it on an empty board |
| Open showcase | Open/close | Open one of the four doors of the vertical showcase. The doors are named from left to right as “first”, “second”, “third”, “fourth”. | The specified door is opened, the robot is static. | open the second door of the showcase |
| Close showcase | Open/close | Close one of the four doors of the vertical showcase that is already open. | The specified door is closed, the robot is static. | close the door of the showcase |
| Open fridge | Open/close | Open the door of the small horizontal ice cream fridge. | The door is open, the robot is static. | open the fridge |
| Close fridge | Open/close | Close the door of the small horizontal ice-cream fridge that is already open. | The door is closed, the robot is static. | close the fridge |

Table 3: Atomic tasks descriptions

| | Pick to basket | From board to board | Pick from floor |
|-------------|--|---|-----------------------------------|
| Train items | Nivea Body Milk Nestle Honey Stars Fanta | Nestle Cereals Duff Beer Can Vanish | Heinz Beans SLAM luncheon meat |
| Test items | Nestle Cereals SLAM luncheon meat | Nivea Body Milk Fanta | Vanish Duff Beer Can |

Table 4: Train/test items split.

2. **Actions**, represented as 11-dimensional vectors:

- 7 values for arm joint positions,
- 1 for gripper control,
- 1 for vertical torso motion,
- 2 for base control: forward/backward linear velocity and rotational velocity around the vertical axis.

We use the Proportional-Derivative (PD) joint position target control mode (referred to as `pd_joint_pos` in ManiSkill3) to control the robot joints, with the exception of the robot base, which is controlled by specifying the linear and angular velocities. The simulator uses these target positions

in combination with a PD controller to compute the torques required to move the joints to the desired positions. Also, we changed joints limits since our motion planning library does not support continuous joints.

B Baselines Fine-tuning

B.1 π_0 and $\pi_{0.5}$

We use the official JAX implementations³ and finetune π_0 and $\pi_{0.5}$ on our dataset using the provided finetuning scripts.

³<https://github.com/Physical-Intelligence/openpi>

| Eval mode | From board to board | | | Open | | Close | | Pick from floor | | Pick to basket | | |
|---------------|---------------------|--------|--------|--------|--------|--------|--------|-----------------|------|----------------|-------|-------|
| | duff | nestle | vanish | fridge | showc. | fridge | showc. | heinz | slam | fanta | nivea | stars |
| Train Seeds | 40 | 30 | 22 | 42 | 2 | 70 | 40 | 52 | 58 | 22 | 34 | 30 |
| In-Domain | 24 | 12 | 4 | 64 | 0 | 60 | 22 | 2 | 2 | 16 | 14 | 22 |
| Unseen Scenes | 6 | 0 | 0 | 20 | 0 | 46 | 28 | 0 | 0 | 2 | 0 | 2 |

Table 5: Average success rates (%) of the generalist VLA model OCTO on atomic retail tasks across different testing scenarios. Higher values indicate better performance.

| Eval mode | From board to board | | | Open | | Close | | Pick from floor | | Pick to basket | | |
|---------------|---------------------|--------|--------|--------|--------|--------|--------|-----------------|------|----------------|-------|-------|
| | duff | nestle | vanish | fridge | showc. | fridge | showc. | heinz | slam | fanta | nivea | stars |
| Train Seeds | 46 | 16 | 18 | 94 | 40 | 98 | 66 | 82 | 72 | 24 | 34 | 22 |
| In-Domain | 22 | 14 | 8 | 92 | 4 | 96 | 70 | 34 | 24 | 20 | 26 | 20 |
| Unseen Scenes | 10 | 2 | 4 | 46 | 4 | 82 | 68 | 18 | 6 | 0 | 0 | 2 |

Table 6: Average success rates (%) of the generalist VLA model π_0 on atomic retail tasks across different testing scenarios. Higher values indicate better performance.

| Eval mode | From board to board | | | Open | | Close | | Pick from floor | | Pick to basket | | |
|---------------|---------------------|--------|--------|--------|--------|--------|--------|-----------------|------|----------------|-------|-------|
| | duff | nestle | vanish | fridge | showc. | fridge | showc. | heinz | slam | fanta | nivea | stars |
| Train Seeds | 86 | 38 | 62 | 98 | 4 | 100 | 78 | 72 | 88 | 62 | 80 | 68 |
| In-Domain | 72 | 52 | 42 | 96 | 4 | 100 | 70 | 48 | 40 | 70 | 62 | 56 |
| Unseen Scenes | 40 | 20 | 6 | 72 | 2 | 88 | 66 | 20 | 2 | 32 | 56 | 26 |

Table 7: Average success rates (%) of the generalist VLA model $\pi_{0.5}$ on atomic retail tasks across different testing scenarios. Higher values indicate better performance.

| Eval mode | From board to board | | Pick from floor | | Pick to basket | |
|-----------------------|---------------------|-------|-----------------|-------|----------------|------|
| | nivea | fanta | duff | fanta | nestle | slam |
| Unseen Scenes & Items | 38 | 8 | 0 | 0 | 20 | 0 |

Table 8: Average success rates (%) of the generalist VLA model $\pi_{0.5}$ on atomic retail tasks for the Unseen Scenes & Items scenario. Higher values indicate better performance.

We opt for full finetuning starting from the provided checkpoints. The AdamW optimizer is used, with the learning rate following a cosine decay schedule, starting at a peak learning rate of $2.5e-5$ and decaying to $2.5e-6$. The batch size is set to 256, and the action horizon is 50. The models are trained to convergence for 75,000 steps on 8xA100 GPUs, which takes approximately 4 days.

B.2 Octo

We employed the official JAX implementation of Octo⁴. We fully finetuned the model following the provided scripts. The model was trained for 1M iterations with a batch size of 128 on 8 A100 GPUs in the multimodal training mode. We finetuned it using 2 history observations and an action horizon of length 4. The finetuning process took approximately 3 days.

⁴<https://github.com/octo-models/octo>

C Evaluation

In Table 5, we report detailed results of the OCTO model evaluation for all tasks and objects. Table 6 shows detailed results of the π_0 model, and Table 7 reports the $\pi_{0.5}$ results. In addition to the “In-Domain” and “Unseen Scenes” scenarios, we also report success rates for the “Train Seeds” scenario, where the models are evaluated on the environments used during training. Table 8 shows results of the $\pi_{0.5}$ model for the “Unseen Scenes & Items” scenario with task-object combinations not seen during training. We do not report analogous tables for OCTO and π_0 as they fail completely in this scenario. We also do not report results for composite tasks, as all models fail in this setup, as shown in the main paper.

Some of the most frequently observed failure modes during model evaluation include:

- Failure to align the gripper with the object, resulting in unsuccessful grasps and the object falling.

- Incorrect object selection, where the robot picks an unintended item.
- Disturbance of surrounding objects, such as knocking down nearby items during execution.
- Successful grasp followed by failure to place the object in the basket.

All evaluations were conducted on a single NVIDIA V100 GPU. The evaluation process for one policy takes approximately one day.

D Additional Simulation Optimizations

Inspired by hierarchical geometric models in computer graphics (Clark 1976), we optimize rendering performance in large-scale store simulations by representing items on shelving units, that are unlikely to be closely observed by the robot, using low-polygon assets obtained through the mesh optimization process described in Section 3.3.

To evaluate the performance gains from our optimization, we conducted the following experiment. We measured simulation time of 50 steps across store scenes with varying numbers of shelving units arranged with various products. In the baseline setup, all shelves used original high-resolution product meshes. In the optimized setup, only the shelf nearest to the robot used original meshes, while all background shelves used downscaled meshes. As shown in Figure 10, optimized scenes yield substantial speedups — for example, simulating 120 shelves with optimized meshes is over three times faster than simulating just four shelves with unoptimized ones. Experiments were conducted on Intel Xeon Gold 6278C CPU and NVIDIA V100 GPU.

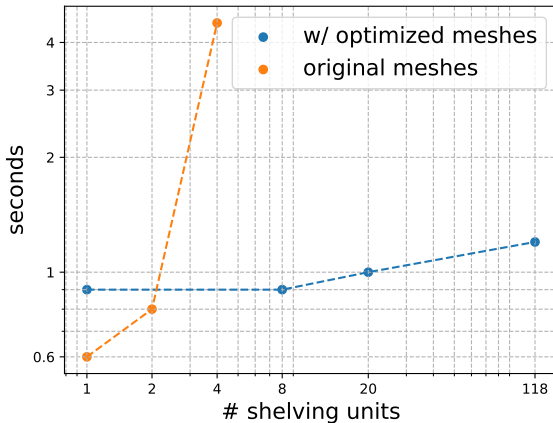


Figure 10: Simulation time for scenes with varying numbers of shelving units arranged with grocery items, comparing items optimized meshes (blue) to original meshes.

Upon visual inspection of multiple rendered scenes from both the ego-view and human camera perspective, we observed that distant geometries appear visually indistinguishable regardless of asset detail level. This supports the use of low-polygon approximations to improve rendering speed

and simulation efficiency. Incorporating dynamic level-of-detail adjustment based on robot or camera pose and field of view is a promising direction for future improvements to the benchmark.

E Access and License

Access RoboBenchMart is publicly available on GitHub: <https://github.com/emb-ai/RoboBenchMart>

License All assets are released under the CC BY-NC 4.0⁵ license, and the codebase under the MIT⁶ license.

⁵<https://creativecommons.org/licenses/by-nc/4.0/deed.en>

⁶<https://opensource.org/license/mit>